

# Microstructural study in graphitised hypereutectoid cast and commercial steels

S. A. Rounaghi\*, P. Shayesteh and A. R. Kiani-Rashid<sup>1</sup>

In the present paper, past research work with new and/or improved processes for willing graphitisation in steels is reviewed. Experiments were carried out to study the carbide dissociation in two different hypereutectoid steels (cast and commercial steels) during graphitisation process by annealing primary martensitic structures at 670°C. Graphite phase evolution during graphitisation treatment was investigated by light optical and scanning electron microscopy and energy dispersive X-ray analyses. It has been reported with promising results that a uniform distribution of alloying elements is found around the graphite particles, which resulted in cast steel. Furthermore, graphite particles in the cast steel were observed to be larger and more spherical than that in commercial steel, which seems to be due to lower Mn/S ratio in cast steel composition.

**Keywords:** Steel, Graphite, Morphology, Phase transformation

## Introduction

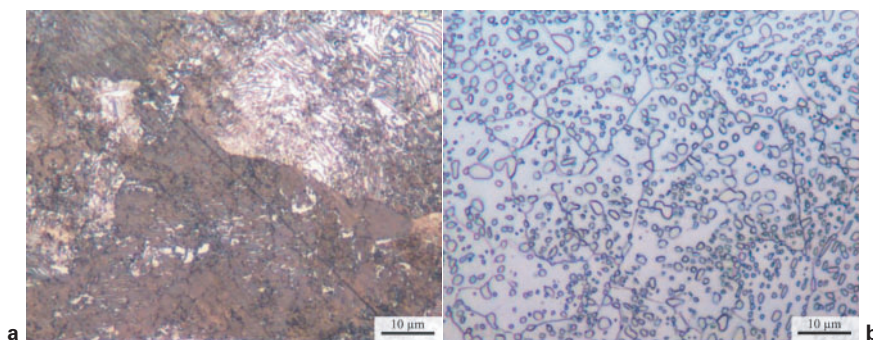
Graphitisation in steels is a solid state phase transformation during a definite heat treatment cycle. It has been reported that the graphite growth in the steels is controlled by the carbon diffusion in ferritic iron. During this diffusion transformation, the semistable cementite phase is decomposed into stable graphite and ferrite phases.<sup>1–4</sup> Graphitisation in steels can be accelerated by annealing from cold worked<sup>5,6</sup> and martensitic<sup>7–9</sup> structures at 600–700°C. Furthermore, fine carbide particles and ferrite grains with high concentration of defects attained from tempered martensitic structure speed up this solid state transformation kinetically.<sup>7</sup>

It has been known that some elements, such as C and Si, in ferrous alloys, are good graphite stabilisers, and others, such as Cr and Mn, are considered as carbide stabilisers.<sup>3,10–12</sup> The effect of these elements can be attributed to accretion or reduction in graphitisation driving force. Therefore, hypereutectoid steels (with higher C content) can be graphitised faster and easier than the hypoeutectoid ones. The preferred microstructure for medium carbon tool steels and low alloy hypereutectoid steels is globular pearlite or spheroidised carbides. The aim of the spheroidising process is to produce a soft structure by changing all hard constituents, like pearlite, bainite and martensite, into a structure of spheroidised carbides in a ferritic matrix, which improves the machinability and cold workability.<sup>13</sup> On the other hand, in nature, graphite is one of the best solid lubricants.<sup>14</sup> The presence of this stable carbon isotope in iron alloys, such as graphitic steels and especially cast

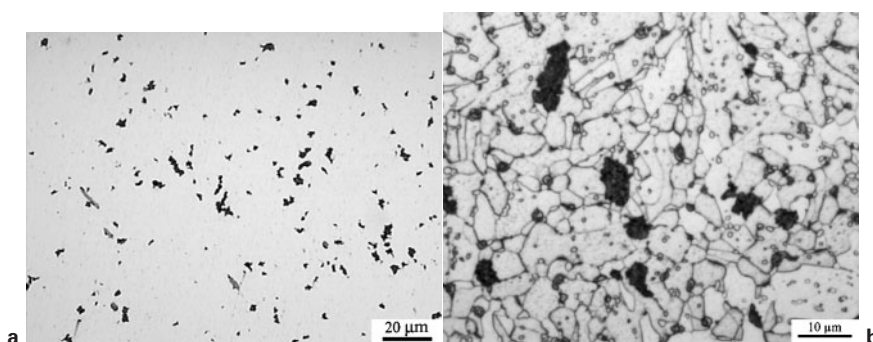
irons, results in the improvement of wear and machining properties of these materials.<sup>10,15,16</sup> Iwamoto and Murakami<sup>17</sup> showed that graphitic steels offer twin of good machinability and cold forgeability rather than conventional steels. Furthermore, by considering the investigations of He *et al.* on medium carbon steels,<sup>8</sup> outstanding results for surpassing graphitisation time have been achieved, which can be interpreted by the effect of adding graphite stabiliser elements such as Si and Al to the steel composition during melting. It should be noted that spheroidising process is usually carried out in higher temperatures and longer time than graphitisation process.<sup>13</sup> Therefore, by reducing graphitisation time twin with good machinability of graphitic steels, they can be considered economically as a competitor of spheroidised hypereutectoid steels. Another important point is the much improvement in mechanical properties such as plasticity and cyclic crack resistance of graphitic steels compared with traditional steels and high strength cast irons.<sup>18,19</sup> In this respect, the authors of this work showed significant improvement in hardness of graphitised structure rather than spheroidised structure by replacing ferritic matrix with hard ones like pearlite, bainite and martensite.<sup>20</sup> Another point that should be mentioned is the dependence of mechanical properties, especially the strength and wear resistance, of cast irons and graphitic steels to morphology and distribution type of graphite in their microstructures.<sup>10,18,21</sup> It has been relevant that transformation of spheroid graphite into vermicular and flake form decreases strength of cast irons and graphitic steels.<sup>10,18</sup> A customary process for changing graphite morphology in cast irons is spheroidising, in which the graphite particles are spheroidised by adding some spheroidised elements such as magnesium and cesium to the melt of grey iron leading to the formation of ductile iron.<sup>22</sup> To classify graphite distribution and morphology in cast irons, some standards are defined by the ASTM.<sup>10</sup>

<sup>1</sup>Department of Materials Engineering, Ferdowsi University of Mashhad, PO Box 91775-1111, Mashhad, Iran

\*Corresponding author, email s.a.rounaghi@gmail.com



1 a microstructure of cast steel after homogenising process and b microstructure of as received commercial steel



2 a as polished micrograph from commercial steel after annealing at 670°C for 60 h and b same structure after etching by 2% nital

The factors which can have an effect on graphite morphology in graphitic steels are still not clear, but electron microscopic observations confirm the role of AlN and BN particles as nucleus for graphite precipitates,<sup>8,23,24</sup> furthermore, irregular morphology of graphite particles which have been formed around these nuclei, has been reported at the early stage of graphitisation.<sup>8,24</sup> In addition, by annealing aluminium treated hypereutectoid steels, a remarkable difference in morphology of graphite phase has been observed (chain- and nodule-like), but the reason for this is unknown.<sup>2</sup> In recent years, some authors<sup>18,19</sup> focused on the effect of the addition of alloying elements, such as copper and aluminium, on graphite morphology in hypereutectoid steels. Their experiments show that Si content up to 2.5 wt-% changes graphite inclusions from quasiglobular to flake or vermicular shape.<sup>19</sup> Similarly, with increasing copper content up to 3.1 wt-%, a gradual change has been observed from spherical to vermicular shape.<sup>18</sup>

Despite performed researches on graphitisation process, the morphology and the distribution of graphite in graphitic steels and related parameters are less mentioned by researchers. For this reason, attempts have been made to prepare steel by alloying the steel via casting using graphitising alloying elements such as silicon. So far, there are some reports in which the graphite phase formed would be totally different from graphitised structures in common commercial steels

during later heat treatment with respect to its morphology, distribution and size.

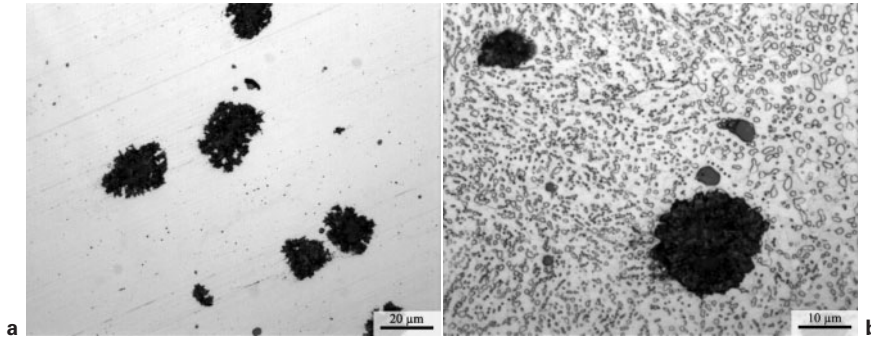
## Experimental

In this research, the graphite formed during heat treatment in commercial hypereutectoid steel (with the composition mentioned in Table 1) is compared to a hypereutectoid cast steel. In order to produce the steel by casting, 15 kg of CK45 steel was charged gradually into the induction furnace. The granular graphite was added to the melt along with ferrosilicon (containing 75 wt-% silicon) before pouring the melt. The addition of granular graphite was carried out in order to increase the carbon content of steel and therefore produce hypereutectoid steel. Furthermore, the addition carbon as the best graphitiser element, can accelerate graphitisation process.<sup>11,18</sup> In addition, ferrosilicon was added in order to decrease the period of the graphitisation transformation.

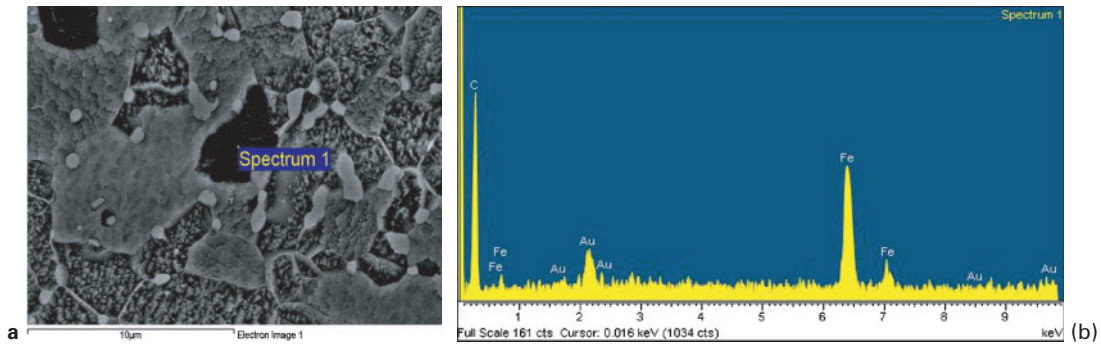
After the addition of the abovementioned materials to the melt, the melt was poured in wet sand moulds. Then, the solidified parts were rejected from the mould. The chemical composition of the cast steel was determined by quantitative analysis according to Table 1. Cast specimens were put inside a container full of cast iron's filings in order to prevent oxidation and decarburising, and then were held at 1100°C for 18 h for homogenising. After this period, they were cooled in air.

Table 1 Chemical composition of commercial and cast steels, wt-%

Steel	C	Si	S	P	Mn	Ni	Cr	Mo	Cu	Al
CK100	0.949	0.213	0.012	0.017	0.339	0.047	0.061	0.008	0.076	0.017
As cast	1.172	1.469	0.026	0.013	0.322	0.079	0.121	0.025	0.189	0.008



3 a as polished micrograph from cast steel after annealing at 670°C for 20 h and b same structure after etching by 2% nital



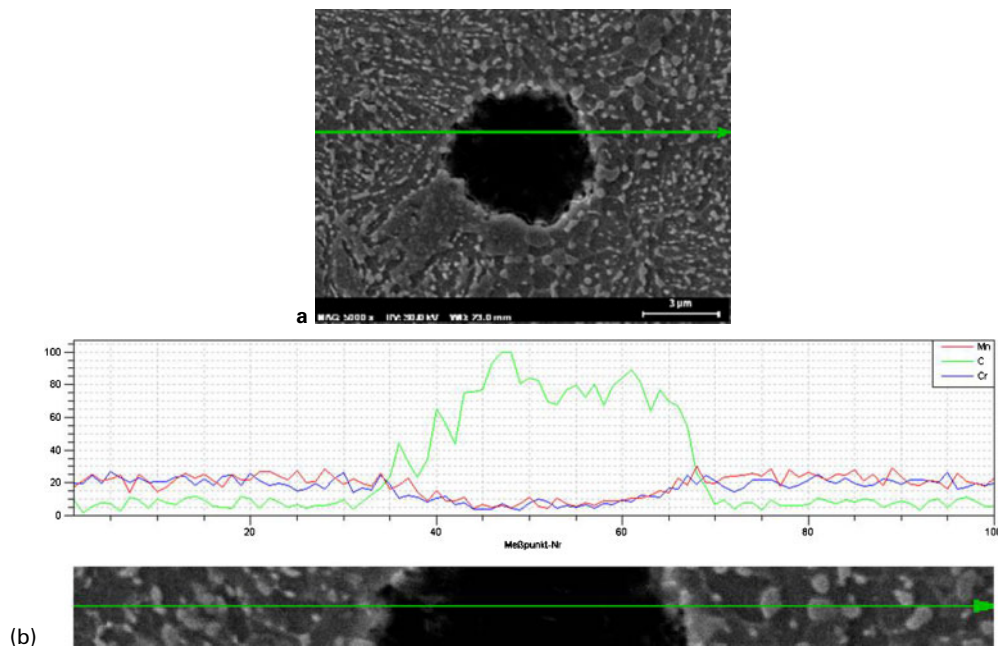
a backscatter electron image of graphite particle; b point scan analyse from this particle

4 Image (SEM) from commercial steel after graphitisation with point scan

In order to form martensitic structure, the homogenised parts were austenitised at 900°C for 20 min along with similar specimens prepared from CK100 commercial steel after being coated with antioxidant/carburising coating (Carbostop). Then, quenching was performed immediately in water at ambient temperature to produce martensitic structure. The aim of graphitisation from martensitic structure is to have a significant reduction in transformation time.<sup>7,8</sup>

For graphitisation, specimens were put inside a container full of cast iron’s filings after recoating with Carbostop. Cast and CK100 specimens were held at 670°C for 20 and 60 h respectively.

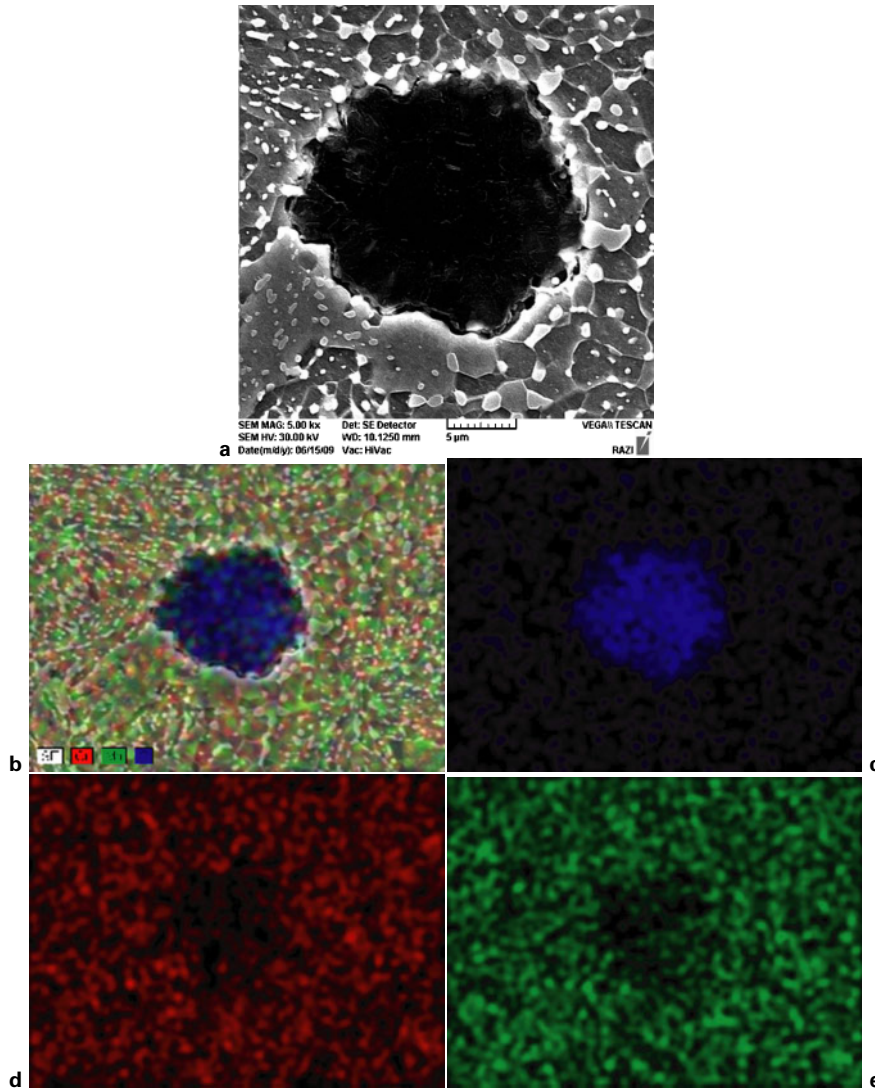
In order to investigate the microstructure using metallographic technique, all of the parts were sectioned in order to prepare microscopic images from their central regions after surface preparation and etching with 2% nital.



a backscatter electron image of graphite nodule; b EDX line scan analysis from this particle

5 Image (SEM) from cast steel after graphitisation with EDX line scan



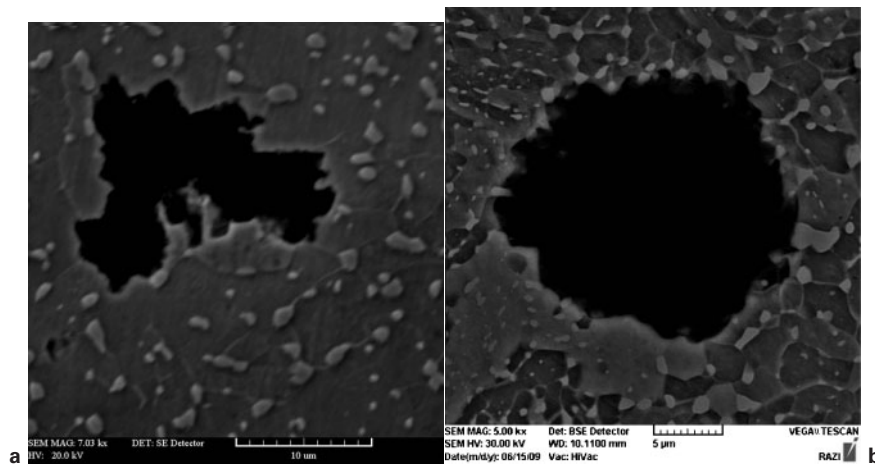


a secondary electron image of graphite nodule; b mapping analysis from this particle; c carbon  $K_{\alpha}$ ; d chromium  $K_{\alpha}$ ; e manganese  $K_{\alpha}$

6 Image (SEM) from graphitised cast steel with mapping

Some of SEM, EDX and mapping images were prepared in Razi Metallurgy Research Center (Tehran, Iran) using a TESCAN machine, and for preparing other images, the scanning electron

microscope model 1450 VP made by Carl Zeiss (Jena, Germany) from the Central Laboratory of Ferdowsi University of Mashhad (Mashhad, Iran) was used.



a commercial steel; b cast steel

7 Image (SEM) from graphitised steels

## Results and discussion

The microstructures of the cast steel after homogenisation and commercial steel are shown in Fig. 1. As seen in this picture, the microstructure of cast steel consists of pearlite and proeutectoid cementite (Fig. 1a). In addition, the initial structure of CK100 commercial steel consists of spherical cementite in a ferritic matrix (Fig. 1b).

Figures 2 and 3 indicate the graphitised structure of the premenioned steels. In order to confirm the presence of graphite, EDX analysis was performed from a graphite particle of the commercial and cast steels separately (Figs. 4 and 5). The Fe peak in EDX spectra analyses may be due to the probably captured iron particles in graphite layers.<sup>25</sup> In some cases, the graphite particles can be dispatched during grinding and polishing so the retained graphite and ferrous matrix can be detected by EDX. For identifying the distribution of alloying elements, mapping and EDX line scan were carried out from a graphite nodule in the cast steel (Figs. 5 and 6).

As can be seen, the carbon peak is identified by EDX in the place of the graphite phase (Figs. 4b and 5b). The per cent of other alloying elements, such as chromium and manganese, is low in these regions due to the presence of carbon in pure state in graphite. However, according to mapping and EDX line scan images, a relative even distribution of these elements is observed in other areas. In addition, based on mapping analysis (Fig. 6d and e) and the findings of other researchers,<sup>8</sup> the probability of the concentration of these elements in residual spherical carbides in the matrix is strengthened.

As can be seen in Figs. 2 and 3, the graphite particles formed in the cast steel are more spherical than commercial ones. In addition, the size of these nodules is much bigger than that of the commercial steel, but they have less and more limited distribution. It should be mentioned that the graphites formed in the cast steel are identical to that of cast iron ( $\sim 10 \mu\text{m}$ ),<sup>26,27</sup> forming a special structure in that steel. Based on the researches performed,<sup>8,17,23</sup> the addition of aluminium and boron to the composition of the steel results in the formation of nitride precipitates, their structures of which are the same as that of graphite. Therefore, the presence of these nitride precipitates in the steel matrix increases the nucleation sites of graphite, leading to their final fine structure.

Since graphitisation periods are not considered identical in these two steels and the chromium content of the cast steel is higher than that of the cast one, according to the effect of this element on the stability of cementite and the decrease in the graphitisation driving force,<sup>12</sup> the decrease in the graphitisation period in the cast steel may not be judged definitely (due to the addition of silicon in comparison with the commercial steel).

The surface area percentages of graphite in the cast and commercial steels were calculated using optical microscopic image analysis as 2.2 and 3.4% respectively. Figure 7 shows SEM images of graphite particles in both of these steels. By comparing these images with ASTM standards in relation to graphite's morphology in cast irons,<sup>10</sup> the shape of graphite in the commercial steel may be considered similar to tempered graphite in malleable iron (type III). On the other hand, the shape of graphite in the cast steel is identical to the spherical

graphite in ductile iron (type I). This difference cannot be attributed to the presence of alloying elements, such as Al and Cu. Yakovlev and Volchok<sup>18</sup> and Ostash *et al.*<sup>19</sup> demonstrated that copper content up to 1.5 wt-% leads to the formation of quasiglobular graphitic inclusions, but Cu content in investigated steels is negligible (Table 1). Simultaneously, the amount of aluminium is so low to have a remarkable effect on graphite morphology.<sup>19</sup> Another point that should be mentioned is the effect of high amount of Si, which can be due to the formation of SiO<sub>2</sub> particles as nuclei for irregular globular graphite particles in cast steel that was reported by He *et al.*<sup>8</sup> Furthermore, the flaked graphite will not be formed in graphitic steels if  $\Sigma(\text{C} + \text{Si}) \leq 3.2\%$ ,<sup>28</sup> which is in good agreement with the authors' observations (Figs. 3 and 4). On the other hand, it has been demonstrated that a lower Mn/S ratio in cast irons leads to the formation of more spherical shape in tempered graphite particles.<sup>10</sup> So far, according to the data listed in Table 1, Mn/S ratios for cast and commercial steels can be calculated as 12.38 and 28.25 respectively. One can generalise the role of Mn/S ratio in cast iron for graphitic steels. In other words, the high difference in the morphology of graphite in these steels may be due to the Mn/S ratio. A similar effect is seen in the studies of Mega *et al.*<sup>24</sup> and Banerjee and Venugopalan,<sup>23</sup> in which Mn/S values can be calculated so high (about 180 and 60 respectively) and irregular morphology of graphite particles has been reported. The same result can be concluded from Mn free graphitic steels<sup>8,29</sup> in which the Mn/S ratio decreases by reduction in the amount of Mn. The dominant form of graphite in these steels is almost spherical.

## Conclusions

1. After graphitisation, the shapes of graphite particles in cast and commercial steels are similar to their morphologies in ductile (type I) and malleable (type III) iron respectively.
2. Graphite particles in the commercial steel are much finer with more distribution in comparison with that in the cast steel.
3. Graphite particles in the cast steel are identical to the particles in cast irons from the point of view of size and distribution.

## Acknowledgements

The authors appreciate Professor Dr A. Zabet and Part Sazan Co. (Tehran, Iran) for preparing some of the light optical microscopic images. In addition, the authors thank Mr G. Isa-Abadi-Bozchelouie for performing some of the tests.

## References

1. H. Sueyoshi and K. Suenaga: *Rev. Soc. Jpn Met.*, 1978, **42**, 676.
2. L. E. Samuels: 'Light optical microscopy of carbon steels', 175–208; 1980, Metals Park, OH, ASM International.
3. K. He, A. Brown, R. Brydson and D. V. Edmonds: *J. Mater. Sci.*, 2006, **41**, 5051–5406.
4. V. I. Bidash and A. I. Prikhod'ko: *Met. Sci. Heat Treat.*, 1987, **29**, 116.
5. M. A. Neri, R. Colás and S. Valtierra: *J. Mater. Eng. Perform.*, 1998, **7**, (4), 467–473.
6. M. A. Neri, R. Colaás and S. Valtierra: *J. Mater. Process. Technol.*, 1998, **83**, (1–3), 142–150.

7. S. A. Rounaghi and A. R. Kiani-Rashid: Proc. 8th Eur. Symp. on 'Martensitic transformation' (ESOMAT), 05018-1-05018-7; 2009, Prague, EDP Science.
8. K. He, H. R. Daniels, A. Brown, R. Brydson and D. V. Edmonds: *Acta Mater.*, 2007, **55**, 2919-2927.
9. A. Rosen and A. Taub: *Acta Metall.*, 1962, **10**, 501.
10. ASM International Handbook Committee: 'Properties and selection: irons, steels, and high-performance alloy', Vol. 1, 13-194; 1998, Materials Park, OH, ASM International.
11. M. Tisza: 'Physical metallurgy for engineers', 338; 2001, Materials Park, OH, ASM International.
12. A. Zhukov: *Met. Sci. Heat Treat.*, 1984, **26**, 849-856.
13. G. E. Totten: 'Steel heat treatment: metallurgy and technologies', 344-349; 2007, Boca Raton, FL, CRC Press.
14. H. O. Pierson: 'Handbook of carbon, graphite, diamond and fullerenes properties, processing and applications', 44-45; 1993, Norwich, NY, William Andrew Inc.
15. S. Katayama and M. Toda: *J. Mater. Process. Technol.*, 1996, **62**, 358-362.
16. H. Klaus: *Giesserei*, 1965, **52**, 583-593.
17. T. Iwamoto and T. Murakami: *JFE GIHO*, 2004, (4), 64-69.
18. A. Y. Yakovlev and I. P. Volchok: *Met. Sci. Heat Treat.*, 2008, **50**, (1-2), 41-43.
19. O. P. Ostash, I. M. Andreiko, I. P. Volchok, I. V. Akimov and Y. V. Holovatyuk: *Mater. Sci.*, 2002, **38**, (6), 765-772.
20. S. A. Rounaghi and A. R. Kiani-Rashid: Proc. 8th Eur. Symp. on 'Martensitic transformation' (ESOMAT), 05017-1-05017-11; 2009, Prague, EDP Science.
21. I. M. Andreiko, I. P. Volchok, O. P. Ostash, I. V. Akimov and Y. V. Holovatyuk: *Mater. Sci.*, 2004, **40**, (3), 416-420.
22. ASM International Handbook Committee: 'Ductile iron', Vol. 15, 'Casting'; 1998, Materials Park, OH, ASM International.
23. K. Banerjee and T. Venugopalan: *Mater. Sci. Technol.*, 2008, **24**, 1174-1178.
24. T. Mega, R. Morimoto, M. Morita and J. I. Shimomura: *Surf. Interface Anal.*, 1996, **24**, (6), 375-379.
25. A. Velichko: 'Quantitative 3D characterization of graphite morphologies in cast iron using FIB microstructure tomography', PhD thesis, University of Saarland, Saarbrücken, Germany, 2008.
26. B. Lux: *AFS Cast Met. Res. J.*, 1972, **8**, 25-38.
27. G. R. Purdy and M. Audier: *Mater. Res. Soc. Symp. Proc.*, 1986, **34**, 13-23.
28. V. M. Zhurakovskii, V. Ya. Sadchikov, N. N. Matveev and G. A. Popkov: *Liteinoe Proizv.*, 1978, (1), 36.
29. K. He, A. Brown, R. Brydson and D. V. Edmonds: *J. Phys., Conf. Ser.*, 2006, **26**, (1), 111-114.